Nanodevice for Imaging Normal Stress Distribution with Application in Sensing Texture and 'Feel' by Touching

Ravi F. Saraf, Vivek Maheshwari
Department of Chemical Engineering, University of Nebraska, Lincoln
rsaraf@unlnotes.unl.edu

Introduction

Touch is one of the five senses designed by nature for survival. 'Touch' may (partially) be characterized as a sensory operation for measuring texture and softness of an object by mechanical contact. We propose to design, fabricate, study and develop, a novel touch sensor made from nanoparticles with broad range of other applications such as, ultrasound medical imaging/diagnostics, smart materials, and non-destructive diagnostics of large structures. The nanodevice is a self-assembled thin-film sensor that will convert static or dynamic (compressive) normal stress distribution to, (i) visible-light, and/or, (ii) electrical current or voltage. The optical and/or electrical signal is proportional to the magnitude of local stress on the sensor's active area. By detecting the light intensity distribution and/or, probing the current distribution on the active area using an electrode array, the stress distribution can be obtained at (potentially) spatial resolution of <10 μm spot. Since the device is self-assembled, the sensor surface can be 100 μm^2 to (in principle) over 1 m^2. Importantly, the dynamic range and the sensitivity of the sensor can be tuned by 1-2 orders of magnitude by regulating the device power supply. Due to high speed (especially for electrical signal), the external stimulus (i.e., stress distribution) may be a pressure or sound radiation. The basic device element is a multilayer film of metallic and (electroluminescent) semiconducting nanoparticles. We have self-assembled a preliminary sensor with active area of 1 cm^2 and sensitivity of ~1 KPa. Since, the total film thickness of the sensor is <100 nm, the normal strain (due to stress) will be highly localized. A patent application on the sensor is filed.

The most successful and conventional sensors used to image pressure and pressure waves (particularly ultrasound) are based on converting mechanical stress to an electrical signal using piezoelectric (1) and magnetorestrictive (2) materials. For sound production and detection for high-resolution imaging (at least above 500 kHz), the more stable and cost-effective pressure imaging methods are based on piezoelectric phenomena. Recently, piezoelectric array transducers have demonstrated great promise in ultra-sound beam forming and imaging capabilities. For ultrasound source, the transducer elements in the array can be weighted and delayed in amplitudes (i.e., phased-array) to produce a wide transmit beam of a precise shape (i.e., apodization), that may be digital-electronically steered and focused at various depths in the sample media (3). These advantages lead to so called parallel processing where sampling in more than one direction and depth can be accomplished simultaneously, thereby improving imaging speed. The effectiveness of piezoelectric based ultrasound systems is remarkable. However such systems are generally non-portable, expensive, and complex. Furthermore, it is difficult to fabricate piezoelectric devices with >100 μm lateral spatial resolution (due to design characteristics such as resonance frequency of the transducer pixel, and inter-transducer acoustic coupling). In particular, for touch-sensor, conformal contact with curved surfaces with

Report Documentation Page

Form Approved
OMB No. 0704-0188

1. REPORT DATE	2. REPORT TYPE	3. DATES COVERED
00 DEC 2004	**N/A**	**-**

4. TITLE AND SUBTITLE	5a. CONTRACT NUMBER
Nanodevice for Imaging Normal Stress Distribution with Application in Sensing Texture and Feel by Touching	5b. GRANT NUMBER
	5c. PROGRAM ELEMENT NUMBER
6. AUTHOR(S)	5d. PROJECT NUMBER
	5e. TASK NUMBER
	5f. WORK UNIT NUMBER
7. PERFORMING ORGANIZATION NAME(S) AND ADDRESS(ES) **Department of Chemical Engineering, University of Nebraska, Lincoln**	8. PERFORMING ORGANIZATION REPORT NUMBER
9. SPONSORING/MONITORING AGENCY NAME(S) AND ADDRESS(ES)	10. SPONSOR/MONITOR'S ACRONYM(S)
	11. SPONSOR/MONITOR'S REPORT NUMBER(S)

12. DISTRIBUTION/AVAILABILITY STATEMENT
Approved for public release, distribution unlimited

13. SUPPLEMENTARY NOTES
See also ADM001736, Proceedings for the Army Science Conference (24th) Held on 29 November - 2 December 2005 in Orlando, Florida. , The original document contains color images.

14. ABSTRACT

15. SUBJECT TERMS

16. SECURITY CLASSIFICATION OF:			17. LIMITATION OF ABSTRACT	18. NUMBER OF PAGES	19a. NAME OF RESPONSIBLE PERSON
a. REPORT	b. ABSTRACT	c. THIS PAGE			
unclassified	**unclassified**	**unclassified**	**UU**	**8**	

complex geometry will be extremely difficult with piezoelectric transducers that are on rigid substrate.

Perhaps, in terms of functionality, the closest sensor to the proposed thin-film device is pressure sensitive paint (PSP). PSP is a promising (pervasive) method with niche application, especially in aerospace industry. PSP contains fluorescent dye that quenches due to oxygen. Since air contains oxygen, the fluorescence is related to the air pressure (4). Since, PSP is an area-active, analog device; the resolution of pressure imaging is high and will be limited only by the optical detection system. However, the sensitivity and application are limited. Since PSP is essentially an oxygen sensor, the application is related to pressure mediated by air (or other oxygen mixture). Furthermore, the optical excitation for fluorescence is necessary, making the implementation and read-out geometry limited to 'open' surface geometries.

The proposed sensor is a nanodevice utilizing Au and semiconducting nanoparticles, that are self-assembled by a techniques that is considered standard today. The advantages of sensor-device using nanoparticle in contrast to current microelectronics approach are several: (i) Small size eliminates phonon-electron coupling that leads to a non-dispersive system. This for example, improves photoluminescence efficiency and high conversion efficiency of electronic signal to light. (ii) Nano-scale systems consume less power. (iii) Quantum confinement effects lead to high tunability of intrinsic material property. For example, the same material can exhibit photoluminescence at different wavelengths depending on particle size. (iv) Possibility of easy processing such as self-assembly in contrast to expensive standard Si (dry) processing methods (photolithography, plasma deposition, etc.).

Several electro-optical and electronic devices utilizing nanoparticles as part of active structure have been fabricated. From the device fabrication complexity point-of-view, they may be categorized in two types: (i) Type I: Only one contact for carrier (electron or hole) injection is important; (ii) Type II: A two point contact across the nanoparticles is critical.

Light emitting diodes (5,6), photovoltaic device (7), capacitor (8), and simple nanoparticle-to-nanoparticle resonance electron transfer by photo excitation (9), are examples of Type I type of systems. In the above device the critical aspect of the active mechanism is transport of charge carrier into the nanoparticle from either a conductive organic thin-film, metal electrode or another particle. For example, one of the first devices demonstrated was a hybrid multiplayer structure composed of In-Sn-Oxide (ITO) electrode/organic semiconducting polymer/inorganic semiconducting nanoparticle/Mg-Ag electrode layers (5). The device can be viewed as two Schottky diodes where the holes are injected into the polymer and electron into the nanoparticle from high work function ITO or Au electrodes (5). As the bias increases the recombination shifts from the nanoparticle into the polymer thereby changing the light emission from red to green. The success of the device indicates that carrier injection into a monolayer of nanoparticle is possible via a metal electrode without shorting.

Single electron transistor (10,11), and single electron tunnel junctions (12), nanoparticle tunnel diode (13), and resonance tunneling devices (14) requiring two contacts across on the same particle are Type II devices. The fabrication of type II devices is more complex since two contacts are required. In all the above reports (10-14) the electrodes were flat electrodes

except for the single electron tunnel junction studies (12) where one of the electrodes is a scanning tunneling microscope (STM) tip. These nanoparticle based devices exhibit all the three types of I-V characteristics observed in lithographically fabricated nanodevices, namely, (i) Coulomb blockade effects where the current 'jumps' at bias voltage difference equal to the charging energy of the nanoparticle; (ii) Stair-case curve, where the current has several smaller jumps corresponding to the discreet unoccupied energy levels; and (iii) Resonance tunneling behavior where a negative resistance behavior is observed. The resonance tunneling behavior manifested as negative resistance is only reported for the InAs based nanoparticle. These devices are kin to more studied lithographically assemble devices that are fabricated by conventional microelectronics method where, an isolated nano-size semiconductor or metallic island (i.e., quantum dot) is deposited such that charge may be injected into the island via a dielectric tunneling barrier (15).

Although the I-V characteristics in nanoparticle-based devices is similar to the lithographically fabricated devices, the discreet electron transfer leading to staircase type I-V curves is weak. In structures fabricated from monolayer of nanoparticles and operating at room temperature the coulomb blockade effect tends to dominate over the discreet electronic states (i.e., stair-case I-V curves) in the <10 nm particle systems studied (for example, references (8), (10) and (13)). These blockade and staircase effects rapidly get weaker at higher temperatures (i.e., room temperature) and for particles above 10 nm (15).

Concept of the Device

The device is a multilayer structure of alternating monolayer of Au and semiconducting nanoparticles spaced with dielectric layers (see Fig. 1). The sensor element is a repetitive stack of a four layer structure comprising of $M/I_1/S/I_2$, where M is layer comprising of metal nanoparticles, S is a layer comprising of a direct band-gap semiconducting nanoparticles and I_1 and I_2 are polymeric dielectric layers. Each metal/insulator/semiconductor stack acts as a Schottky diode (16) with a barrier at the semiconductor/insulator interface. In Fig. 1, the current is from bottom to top or the electrons are traversing from top to bottom. As is the case for the device discussed, we consider the semiconducting nanoparticle to be an n-type material. For the applied bias voltage shown, (from the top), $M/I_1/S$ and $S/I_2/M$ Schottky diodes are in reverse and forward bias, respectively. In principle, the two dielectric layers, I_1 & I_2 of thickness, δ_r & δ_f, respectively, are different. The difference in the dielectrics can be tailored by either controlling the material composition and/or thickness.

As a normal force is applied, the thickness of insulation tunneling barrier decreases causing the internal field in the layer to increase leading to a higher Schottky barrier. Since CdS is an n-type semiconductor, the electron transport in forward and reverse bias diodes will decrease. However, the minority carriers, the hole-current transport that governs the output light will increase. In the elastic regime (the case for this study), the strain in the film is proportional to applied stress. Thus, by measuring the electric current (Electrical device) or; (ii) the intensity of electroluminescent light (Optical device); a sensitive measure of local pressure is obtained. Since, the level of signal increases with the applied bias, the dynamic range can be tuned by regulating the bias.

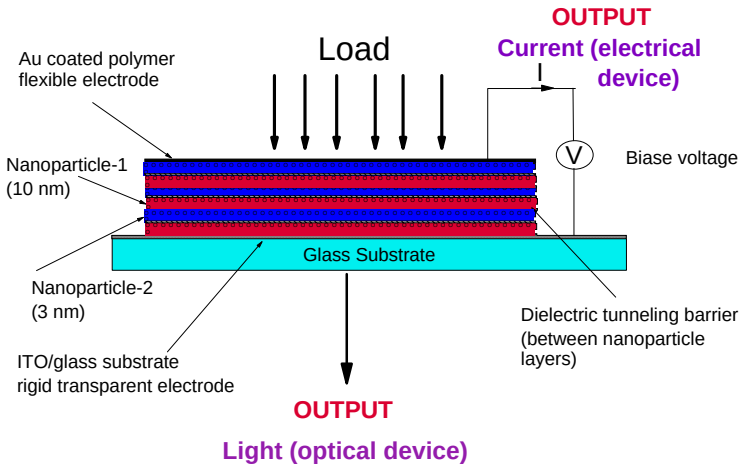

Fig. 1: Schematic of the sensor indicating two types of nanoparticle monolayers: Au and CdS. The bottom electrode on a solid substrate is Indium-Tin-Oxide (ITO), a transparent, conducting, material. The top electrode is Au on a flexible film such that the applied load strains the film corresponding to local stress. The applied load may be measured by a visible light signal (image view) or electrical current, I. Thin dielectric layer separates the nanoparticle monolayers from each other.

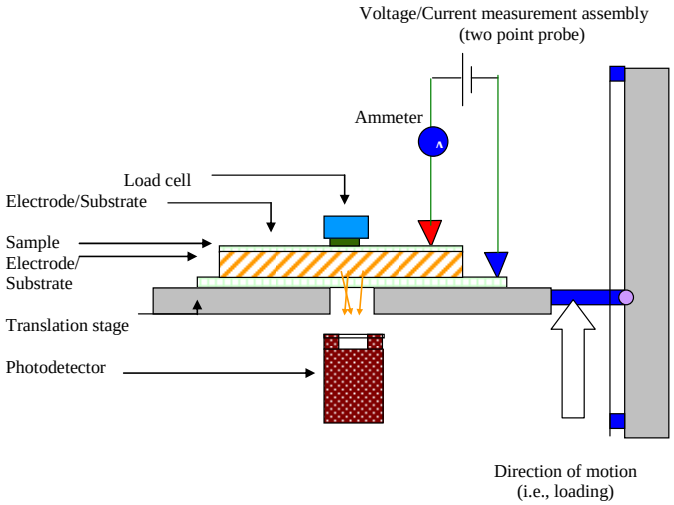

Fig. 2: The sample on transparent ITO electrode containing substrate (labeled as Electrode/Substrate) is placed on a platform that moves in the vertical direction as indicated. Due to the vertical motion, the sample is compressed between the substrate and Au coated load cell plate. The I-V curve across the sample thickness is measured by probing the ITO and au electrode as shown. The light output is collected through the transparent ITO electrode.

Results and Discussion

Fig. 2 shows the schematic to study the characteristics of the device. Both electroluminescence and current are measured simultaneously as a function of applied load and bias voltage. The sample is placed on a translation stage that is attached to a platform that can be moved by a computer driven precession motor. As the platform is vertically moved, the sample is compressed between the load cell plate and the substrate. The load cell measures the compressive force, F. A two-point probe measures an I-V curve at each compressive load. Since the currents can be very low, over 25 points are measured at each bias voltage. Thus I (signal) vs V (bias) characteristics at family of compressive force are obtained. The data is then transposed to obtain I (signal) versus compressive stress, σ = F/(sample area) at various V (bias). Simultaneously, the electroluminescence is measured for each bias voltage and F (or σ). The detector output is analog. Statistics is obtained by recording the detector signal every 1-10 ms. Fig. 3 shows the actual set-up. The computer monitor is 21" and the digital load monitor is about 3" across.

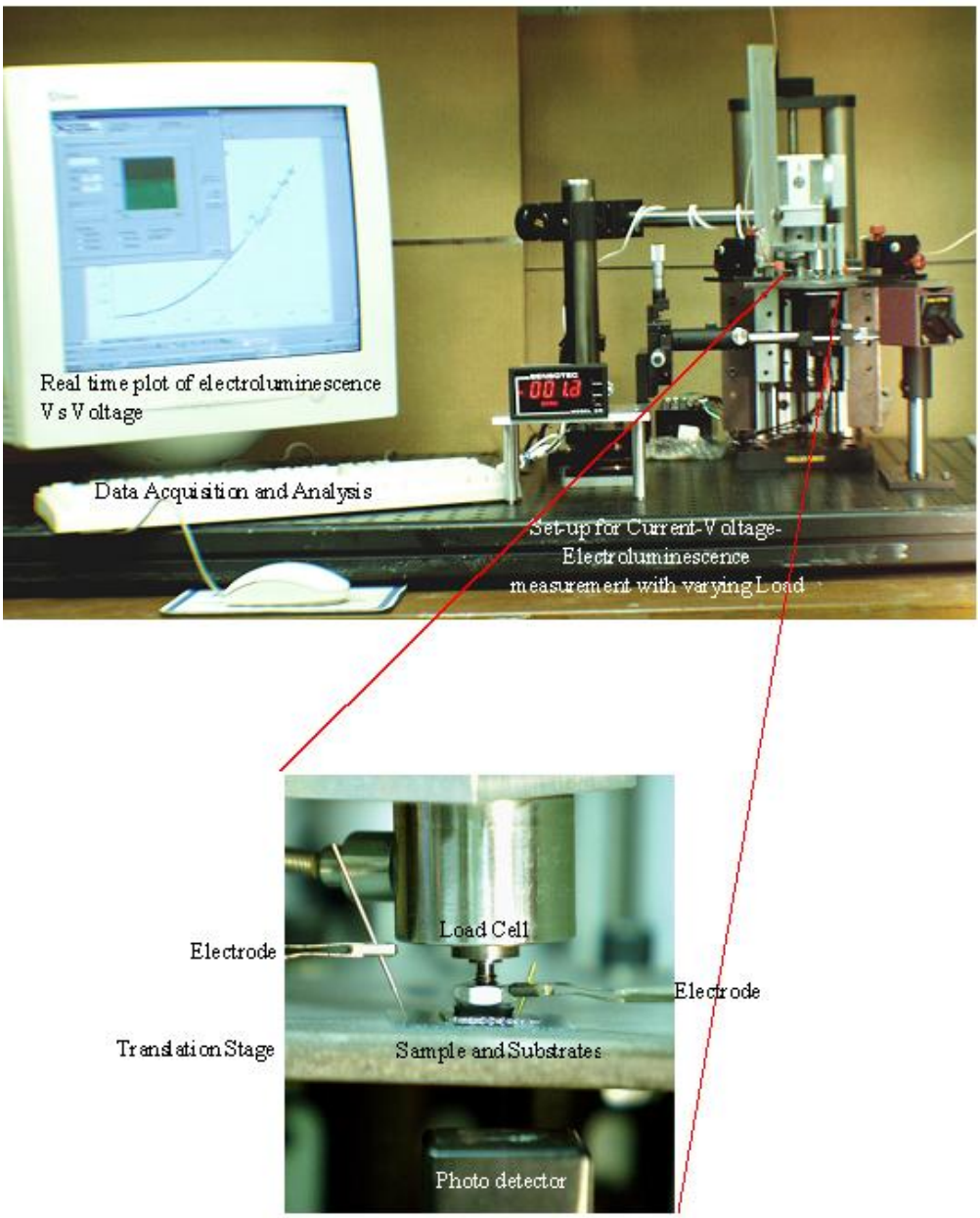

Fig. 3: Photograph of the device performance set-up. The system is designed, fabricated, assembled, and completely automated in-house. The blow-up shows the device location with Ta electrodes and the load cell. The thick substrate above the photodetector is ITO coated glass.

The electrical and optical performance is measured on a 37-layer structure composed of 3 layers of Au nanoparticles, 2 (double layers) of CdS nanoparticles that are each spaced by 6 monolayer of polymer. Fig. 4 shows the simultaneous measurement of current and electroluminescence intensity in the apparatus shown in Fig. 3.

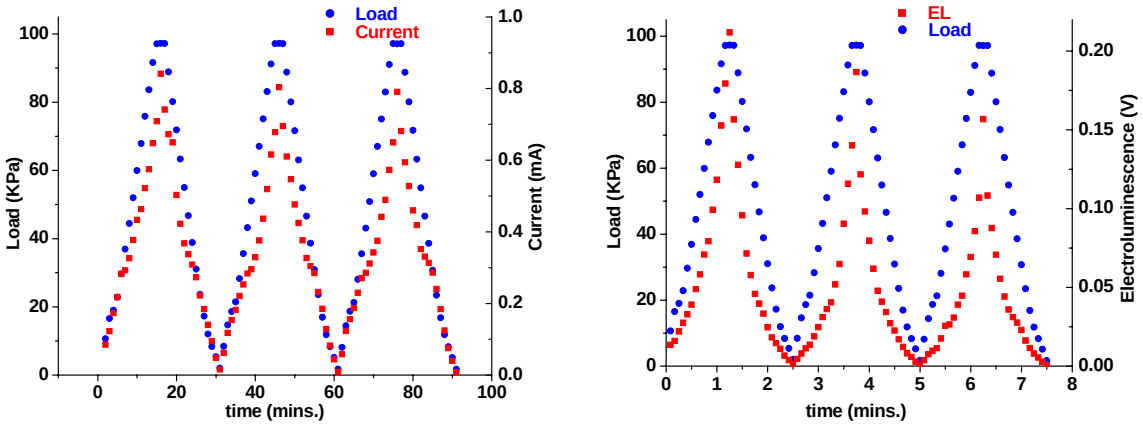

Fig. 4: Characteristics of the device under cyclic load. The applied bias is 20 V.

The current and electroluminescence tracks the load well for 2-3 cycles. The small decay in the electroluminescence signal occurs due to charging (i.e., capacitance) effects. The original signal is recovered on grounding the device before subsequent run. Furthermore, consistent with theory (not discussed in this report), the current and electroluminescence are linear with respect to applied load.

The efficiency of the device is proportional to the ratio of measured electroluminescence intensity divided by the current; i.e., the fraction of electrons transported into the CdS particle that produce photons. Fig. 5 show the efficiency of the device. Since the slope is constant for each of the two curves at 8 and 10V, the efficiency of the device is constant. The highest electroluminescence data point for each bias corresponds to 10 KPa load. Thus, the electroluminescence signal increases by ~6 folds by increasing the bias just by 2 V. This indicates that the bias can effectively regulate the dynamic range (and sensitivity) of the device.

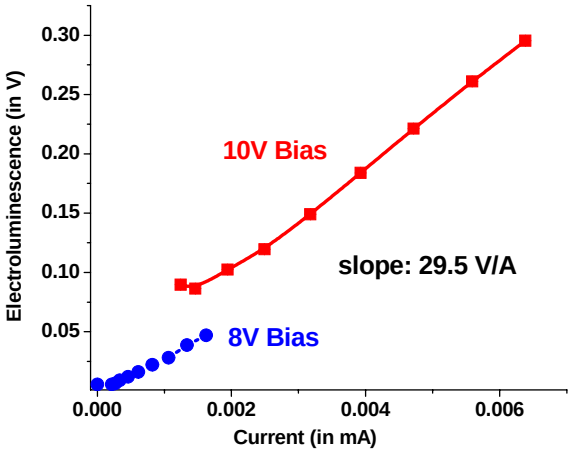

Fig. 5: Efficiency of the device over a loading from 0 to 10 KPa at a constant bias of 8 and 10 V. Both the lines are linear fit with fitness better than 95%. The lines pass through the origin. The slope proportional to efficiency is same for the two biases. The electroluminescence signal for 10 KPa load increase by ~6 folds as the bias is increased from 8 to 10 V.

Pressure imaging

To create a pressure distribution, a ~ 3 mm radius bead was placed on the device and pressed with a soft polymer plate. To measure the intensity distribution, light was collected below the device through a 20X objective with a spot size of 20 μm and numerical aperture of 0.22. The

objective was scanned to obtain the electroluminescence intensity distribution as a function of displacement of the objective. The objective was scanned by a stepper motor.

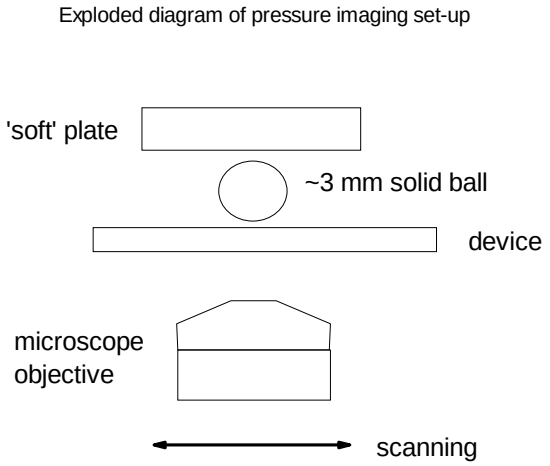

Fig. 6: Setup to measure the electroluminescence from non-uniform loading. The loading is spatially changed by incorporating ~3 mm radius plastic beads. The light output is measured by focusing on the sample plane. The spot size is ~20 μm.

Fig. 7 shows the scanned image across a bead. We show a scan with the largest spread, i.e., along the diameter of the bead. The shape is Gaussian and the integral full width is about the size of the bead indicating that the device can image pressure distribution.

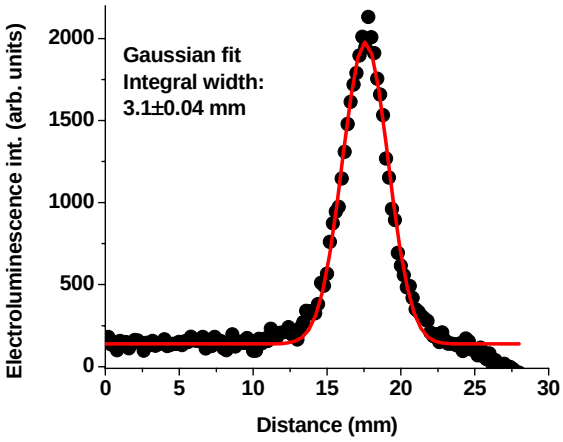

Fig. 7: One dimensional scan of pressure distribution from ~3 mm compliant bead.

Conclusion and summary

We have demonstrated a large area, self-assembled device composed of nanoparticle to convert pressure into an electrical and/or an optical signal. The characteristics of the device agrees with theoretical predictions. The low hysterisis on cyclic load indicates excellent charge balance of majority and minority currents through the nanoparticles. The device fabricated is a 37 layer structure over 1 cm^2 area. Since, the device is by self-assembly and fabricated under ambient conditions, very large area pressure imaging sensors can be manufactured by this approach. The device has several applications, such as smart bed sensor, sound and pressure imaging.

References

1. D.J. Jones, S.E. Prasead, J.B. Wallace, *Piezoelectric materials and their applications*, Adv. Ceramic Mat., 122, 71 **(1996).**
2. P. Squire, *Magnetostrictive materials for sensors and actuators,* Ferroelectrics, 228, 305 **(1999**).
3. For a recent account on new developments in ultrasound technology for imaging and beam control and conditioning see, Ultrasound in Medicine, Eds. F.A. Duck, A.C. Baker, H.C. Starritt, IOP Publ., London **(1998)**.
4. B.G. McLachlan, J.H. Bell, *Pressure Sensitive Paint in Aerodynamic testing,* Expt. Therm. Fluid Sci., **10,** 470-485 **(1995)**.
5. V.L. Colvin, M.C. Schlamp, A.P. Alivisatos, Light-emitting Diodes made from Cadmium Selenide Nanocrystals and Semiconducting Polymer, Nature, 370, 354-357 **(1994)**.
6. K.S. Narayan, A.G. Manoj, J. Nanda, D.D. Sarma, *Dual Function Hybrid Polymer-nanoparticle Devices,* Appl. Phys. Lett., 74, 871-873 **(1999)**.
7. N.C. Greenham, X. Peng, A.P. Alivisatos, Charge Separation and Transport in Conjugated-polymer/semiconductor-nanocrystal Composites Studied by Photoluminescence Quenching and Photoconductivity, Phys. Rev. B., 54, 17628-17637 **(1996)**.
8. G. Markovich, D.V. Leff, S.-W. Chung, H. Soyez, B. Dunn, J.R. Heath, Parallel Fabrication and Single-electron Charging of Devices Based on Ordered, Two-dimensional Phases of Organically Functionalized Metal Nanocrystals, Appl. Phys. Lett., 70, 3107-3109 **(1997)**.
9. C.R. Kagen, C.B. Murray, M.Nirmal, M.G. Bawendi, *Electronic Energy Transfer in CdSe Quantum Dot Solids,* Phys. Rev. Lett., 76, 1517-1520 **(1996)**.
10. D.L. Klein, R. Roth, A.K.L. Lim, A.P. Alivisatos, P.L. McEuen, *A Single-electron Transistor from Cadmium Selenide Nanocrystal*, Nature, 389, 699-701 **(1997)**.
11. S.H.M. Persson, L. Olofsson, L. Gunnarsson, Appl. Phys. Lett., 74, 2546 **(1999)**.
12. B. Alperson, S. Cohen, I. Rubenstein, G. Hodes, Phys. Rev. B., 52, 17017 **(1995)**.
13. S.-H Kim, G. Markovich, S. Rezvani, S.H. Choi, K.L. Wang, J.R. Heath, *Tunnel Diodes Fabricated from CdSe Nanocrystal Monolayers,* Appl. Phys. Let., 74, 317-319 **(1999)**.
14. SK Jung, SH Song, SW Hwang, JH Park, Y, Kim, EK Kim, Fabrication and Electrical Characterization of Planar Resonant Tunneling Device incorporating InAs Self-assembled Quantum Dots, Physica B, 272, 18-20 **(1999)**.
15. KK Likharev, *Single-Electron Devices and Their Applications,* Proceedings of the IEEE, 87, 606-632 **(1999)**.
16. S.M. Sze, *Semiconductor Devices: Physics and Technology*, J. Wiley & Sons, New York (1985), p.160-171.